Eur. Phys. J. AP **9**, 153–163 (2000)

THE EUROPEAN PHYSICAL JOURNAL APPLIED PHYSICS

An inverse technique to deduce the elasticity of a large artery

P.-Y. Lagrée[a]

Laboratoire de Modélisation en Mécanique, Université Paris VI, UMR 7607, B.P. 162, 4 place Jussieu, 75005 Paris, France

Received: 22 January 1999 / Revised: 9 December 1999 / Accepted: 14 December 1999

Abstract. Our purpose is to build an inverse method which best fits a model of artery flow and experimental measurements (we assume that we are able to measure the displacement of the artery as a function of time at three stations). Having no clinical data, we simulate these measurements with the numerical computations from a "boundary layer" code. First, we revisit the system of Ling and Atabek of boundary layer type for the transmission of a pressure pulse in the arterial system for the case of an elastic wall (but we solve it without any simplification in the $u\partial u/\partial x$ term). Then, using a method analogous to the well known Von Kármán-Pohlhausen method from aeronautics but transposed here for a pulsatile flow, we build a system of three coupled non-linear partial differential equations depending only on time and axial co-ordinate. This system governs the dynamics of internal artery radius, centre velocity and a quantity related to the presence of viscous effects. These two methods give nearly the same numerical results. Second, we construct an inverse method: the aim is to find for the simple integral model, the physical parameters to put in the "boundary layer" code (simulating clinical data). This is done by varying in the integral model the viscosity and elasticity in order to fit best with the data. To achieve this in a rational way, we have to minimise a cost function, which involves the computation of the adjoint system of the integral method. The good set of parameters (*i.e.* viscosity, and two coefficients of a wall law) is effectively found again. It opens the perspective for application in real clinical cases of this new non-invasive method for evaluating the viscosity of the flow and elasticity of the wall.

PACS. 47.15.-x Laminar flows – 47.60.+i Flows in ducts, channels, nozzles, and conduits

1 Nomenclature

u longitudinal velocity
v transversal velocity
h displacement of the artery radius
p pressure
x longitudinal variable
r radial transversal variable
η reduced variable r/R
t time
R artery radius
R_0 unperturbed artery radius
α Womersley number
ω pulsation
k elasticity of the wall
$\bar{k}_1$, $\bar{k}_2$ adimensionalized coefficient of elasticity
U_0 velocity at the center of the pipe
Q the flux
q defect of flux: an integral linked with u
Γ an integral linked with u^2
τ coefficients of skin friction
γ coefficients of Γ
δR the gauge of h
L the longitudinal scale
ε_1 a small parameter R/L
ε_2 a parameter $\delta R/R$
ε_{n} amplitude of random noise
J the cost function
J_0 Bessel function of order 0
J_1 Bessel function of order 1
* adjoint variables
$\mathfrak{L}$ the Lagrangian.

2 Introduction

Numerical computation of blood propagation in arteries is a great challenge for mechanics: it involves an unsteady 3D motion of a complex non-homogenous non-Newtonian fluid interacting with a moving changing shape 3D geometry. Most of the physical parameters involved are unknown or difficult to measure, numerical methods are under development but computers are not powerful enough. Mathematical settlements of convergence of the process are not completely established (Errate *et al.* [7]). Nevertheless, many examples of successful computations with simple descriptions of the fluid and/or the wall can be found in the literature. Among them, Reuderink *et al.* [26] use the linear wave propagation of the small disturbance as boundary conditions for a full Newtonian Navier Stokes

[a] e-mail: pyl@ccr.jussieu.fr

computation, the input being a sinusoidal pulse (to compare with Womersley [38] results). Vesier and Yoganathan [35] present a real interaction between a full Newtonian axial-symmetric Navier Stokes code and an elastic wall (string law and no inertia), the input being a sinusoidal pulse again. Ma, Lee and Wu [17] (first models are in Wu, Lee and Tseng [17] and Wu and Lee [17]) present a computation with full Newtonian axi-symmetrical Navier Stokes code with a refined description of the wall displacement (though finally linearized). Effects of cross-section change with a rigid wall are computed by Pedrizzetti [22].

When the phenomena in the wall were emphasised (inertia, axial and longitudinal tension, viscoelasticity, etc.) the flow was simplified. The velocity is supposed to be constant over the section and the viscous effect is a friction force (Seymour [30] studied the competition between dissipation and non-linear effects in the propagation of a monochromatic flow). The flow is often even linearized as in Kuiken [10] though it remains viscous, or it is taken as a perfect fluid though it remains non-linear as in Yomosa [42] or in Paquerot and Remoissenet [21] (in the two last references non-linearity and dispersion lead to solitons).

Nevertheless, most of the operational techniques use a simplified set of equations for the fluid and for the wall: the equations are averaged on the section and the skin friction (which appears during the integration over the section) is modeled by a "closure" relation involving the flux and the viscosity (deduced from the guessed velocity profile). See for example Pedley [23], Zagzoule and Marc-Vergnes [44], Horsten *et al.* [12], Zagzoule, Khalid-Naciri and Mauss [43], Mederic, Gaudu, Mauss and Zagzoule [18], Yama, Mederic and Zagzoule [41], Rogova and Flaud [27], Pythoud Stergiopulos and Meister [25] or to a certain extent Belardinelli and Cavalcanti [2].

These methods, based on drastic simplifications of the complete equations system, are powerful in large arteries. This is due to the fact that the dominant mechanism, as explained by Lighthill [15] and Pedley [23], involves the propagation of a rather small amplitude pressure wave and that the viscosity and the viscoelasticity are not particularly dissipative. So, here we adopt a simple point of view and simplify the full Navier Stokes equations; we use a kind of boundary layer (or thin layer) approach of the equations and work with the Ling and Atabek [16] system (referred as "boundary layer system"). Simplifying much more, in the spirit of the preceding references, we will integrate these equations transversally and use a closure from the Womersley [38] linear solution (the result is referred as "integral system"). Comparisons between numerical simulations of the final integral system and of the original boundary layer system (without any simplification such as the k function of Ling and Atabek [16]) are exposed, and we shall see that they are similar in linear and non-linear cases.

The main reason for the interest in the flow in an elastic pipe is the belief that it may help to understand a pathological state of an artery. In this scope, an interesting tool would be to measure the elasticity (or the compliance) of the wall *in vivo,* in a non-invasive way to predict or follow the evolution of diseases (or we may want to study how to develop a prosthesis for a femoral artery). The idea is that we have a simplified model (depending on a set of coefficients, in this case the viscosity and the linear compliance of the wall, but other parameters may be put in the model) and we want the set of coefficients which describes best the experiments. Our aim is different from Rogova and Flaud's [27] and from Pythoud, Stergiopulos and Meister's [25], who are interested in separating the forward and backward waves, but we also use a simplified integral model for the flow. We suppose that it is possible (we do not discuss the experimental difficulties and precision problem) to obtain from Doppler measurements the displacement (or the pressure) at three different locations $x_{\rm in} < x_{\rm m} < x_{\rm out}$, as a function of time (during a period). Two preceding papers ([27] and [25]) need measurements of pressure and velocity at one location. The measured displacements $h_{\rm in}(t)$ and $h_{\rm out}(t)$ are then the boundary conditions for the simplified integral model, $h_{\rm m}(t)$ is compared to the numerically computed result (from the integral model) of the displacement obtained in $x_{\rm m}$; the aim is to find out the set of parameters which makes the measurement and the computation the closest. The so called "inverse method" (Chavent [3]) allows us to construct efficiently such a method. Therefore, we build a cost function which has to be minimised with the help of the numerical resolution of the integral system's adjoint system which allows us to compute the gradient of this cost function.

These methods of back propagation were first developed in seismography in order to "guess" the internal structure of the earth and the location of an earthquake knowing only the seismic measurements (Tarantola [31]). More generally, any complex system may be modelled by a more simple set of coupled O.D.E. or P.D.E. depending on a set of parameters, the inverse method leading to the set of optimum parameters. Among others, we may quote the interaction of the wakes (Kármán streets) which are issued from a row of cylinders (Fullana *et al.* [9]), or Barros [1] where the coefficient of friction at the river bed is deduced from measurements of the water level. Having up to now no experimental results, we shall use our thin layer resolution of the Ling and Atabek's system as the "experiment", and our integral description as the model to adjust. So we shall show that the optimum set of parameters found for the integral method are not too far from the "real" ones put in the thin layer resolution, opening the way to future more complex modelling and to real comparisons with clinical data.

3 Dynamical model

3.1 Analysis

An homogenous, Newtonian, incompressible (with constant density ρ) fluid is assumed, the viscosity μ is constant ($\nu = \mu/\rho$); these hypotheses may be relevant for blood if the arteries are wide enough and if we assume that the non-Newtonian behaviour (viscoelasticity) and the fact that blood is a suspension of cells (deformable

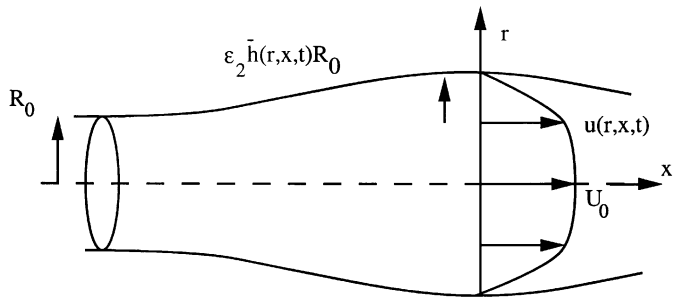

Fig. 1. the flow in the elastic pipe.

solid objects) are negligible. To a certain extent ν and ρ may be taken as re-normalised values (Flaud et Quemada [8]). The flow is assumed to be axisymmetrical, gravity effects are neglected. It is described by the longitudinal $u(r,x,t)$ and the radial $v(r,x,t)$ components of the velocity $\mathbf{u}$. The pressure in the fluid is $p(r,x,t)$. The problem is then to solve the Navier-Stokes equations (for the fluid):

$$\boldsymbol{\nabla}\cdot\mathbf{u}=0 \qquad \text{and} \qquad \frac{\partial\mathbf{u}}{\partial t}+\mathbf{u}\cdot\boldsymbol{\nabla}\mathbf{u}=-\frac{\boldsymbol{\nabla}p}{\rho}+\nu\boldsymbol{\nabla}^2\mathbf{u}. \tag{1}$$

This set of equations is coupled with the artery motion equations (we do not write the general equations for the solid, called the "wall"). The most general boundary conditions are the equality of the velocities at the wall (no slip condition) and the equality of the stresses at the wall. This set of equations has been solved by Vesier and Yoganathan [35] or Ma, Lee and Wu [17] (some mathematical difficulties were shown by Errate *et al.* [7]). But here our scope is to obtain a simplified system for quick resolution with small numerical facilities.

In Figure 1, we present a rough sketch of the notations. As usual, we introduce by phenomenological analysis, small parameters to simplify the equations. First, the no slip condition at the wall $r=R(x,t)$ is simplified as follows:

$$v(r,x,t)|_{r=R}=\frac{\partial R}{\partial t}, \qquad u(r,x,t)|_{r=R}=0. \tag{2}$$

This dictates only radial movements: this is not the most general boundary condition (Womersley [38] retains the two displacements). The wall is tethered to its stiffer surroundings: it seems to be very difficult in practice, to measure this displacement. The pressure is scaled by the elasticity of the wall: if the wall is moved by an amount δR from the equilibrium radius R_0 (roughly about 0.5 cm, and $\delta R/R_0$ is much smaller than 0.1), the simplest expression for the restoring pressure is $k(\delta R)$ (roughly about $13k$ Pa). With the same scale δR for the variations of the radius and with T the period of blood ejection (characteristic time $T\simeq 1.2$ s), we scale the transverse velocity by $\delta R/T$. Given L, a characteristic length, and u_0, a characteristic longitudinal velocity (up to now unknown), and noticing that transverse variations are scaled by R_0, the incompressibility imposes $u_0\sim L(\delta R/R_0)/T$, and the longitudinal momentum $\rho u_0/T\sim k(\delta R)/L$. Hence a good possible choice for L is $T\sqrt{\frac{kR_0}{\rho}}$ and for u_0 $\frac{\delta R}{R_0}\sqrt{\frac{kR_0}{\rho}}$(note $c_0=\sqrt{\frac{1}{2}}\sqrt{\frac{kR_0}{\rho}}$ is known as the Moens-Korteweg celerity and the value is about 3 to 10 m/s), other good choices for scales are linked to this one (except factors π or $\sqrt{2}$).

The preceding scales define an adimensionalized parameter that we may call $\varepsilon_2=\frac{\delta R}{R_0}$. It measures the importance of the non-linearity in the fluid ($(\mathbf{u}\cdot\boldsymbol{\nabla})/(\frac{\partial}{\partial t})=O(\varepsilon_2)$) as well as in the wall. This parameter is typically much smaller than 0.1. The ratio $\varepsilon_1=\frac{R_0}{L}$ is in practice smaller than 10^{-2}, enabling the transverse variation of pressure to be neglected, which is of the order of ε_1^2. Finally, the relative importance of viscosity is related to the ratio of the viscous term by the unsteady term: $(\nu u_0/R^2)/(u_0/T)$. This permits us to define the classical Womersley number $\alpha=R_0\sqrt{\frac{2\pi/T}{\nu}}$. The bigger α, the flatter the velocity profile; the smaller α, the better we obtain a Hagen-Poiseuille flow. We shall consider that in practice (for femoral arteries) α is between 3 and 5. The longitudinal derivative viscous term is of course ε_1^2 smaller than the transversal one. Finally, we must mention the Reynolds number, though for this unsteady flow the Womersley number is more relevant. The Reynolds number constructed with the diameter is $R_{eD}=(u_0(2R_0))/\nu$. After substitution this is $R_{eD}=\pi^{-1}\varepsilon_2\varepsilon_1^{-1}\alpha^2$ which is at most 100.

3.2 Final form for the fluid

With the following adimensionalization:

$$x=T\sqrt{\tfrac{(kR_0)}{\rho}}\bar{x},\ r=R_0\bar{r}, \quad t=T\bar{t}$$
$$u=\varepsilon_2\sqrt{\tfrac{(kR_0)}{\rho}}\bar{u},\ v=\varepsilon_2\tfrac{R_0}{T}\bar{v},\ p=\varepsilon_2(kR_0)\bar{p},\ R=R_0\bar{R},$$

where $c_0=\sqrt{\frac{1}{2}\frac{kR_0}{\rho}}$ and $\varepsilon_1=\frac{R_0}{L}$, $\varepsilon_2=\frac{\delta R}{R_0}$ and $\alpha=R_0\sqrt{\frac{2\pi/T}{\nu}}$, we write again the system (1). As the boundary conditions are evaluated on a moving unknown surface (the location of the wall is $\bar{r}=\bar{R}(x,t)$) we map the equations in introducing a new variable: $\bar{\eta}=\bar{r}/\bar{R}(\bar{x},\bar{t})$. The boundary conditions are then on a fixed surface: $\bar{\eta}=1$, but it introduces new terms in the equations (*e.g.* the $\partial/\partial\bar{t}$ term is now $\partial/\partial\bar{t}-(\bar{\eta}/\bar{R})(\partial\bar{R}/\partial\bar{t})\partial/\partial\bar{\eta}$ and so on). As ε_1 is the real small parameter (ε_2 is not necessarily small, and α not necessarily large), we obtain a boundary layer like system of equations:

$$\bar{R}=1+\varepsilon_2\bar{h}$$
$$\frac{1}{R}\frac{\partial\bar{v}}{\partial\bar{\eta}}+\frac{\bar{v}}{\bar{\eta}\bar{R}}+\frac{\partial\bar{u}}{\partial\bar{x}}-\varepsilon_2\cdot\frac{\bar{\eta}}{\bar{R}}\frac{\partial\bar{R}}{\partial\bar{x}}\frac{\partial\bar{u}}{\partial\bar{\eta}}=0, \tag{3}$$

$$\frac{\partial \bar{u}}{\partial \bar{t}} - \varepsilon_2 \cdot \frac{\bar{\eta}}{\bar{R}} \cdot \frac{\partial \bar{h}}{\partial \bar{t}} \cdot \frac{\partial \bar{u}}{\partial \bar{\eta}} + \varepsilon_2 \left(\frac{\bar{u}}{\bar{R}} \cdot \frac{\partial \bar{u}}{\partial \bar{\eta}} + \bar{u} \left(\frac{\partial \bar{u}}{\partial \bar{x}} - \varepsilon_2 \frac{\bar{\eta}}{\bar{R}} \cdot \frac{\partial \bar{h}}{\partial \bar{x}} \cdot \frac{\partial \bar{u}}{\partial \bar{\eta}} \right) \right) = -\frac{\partial \bar{p}}{\partial \bar{x}} + \frac{2\pi}{\alpha^2} \left(\frac{1}{\bar{\eta}\bar{R}^2} \cdot \frac{\partial}{\partial \bar{\eta}} (\bar{\eta} \frac{\partial \bar{u}}{\partial \bar{\eta}}) + O(\varepsilon_1^2) \right), \quad (4)$$

$$\frac{\partial \bar{p}}{\partial \bar{\eta}} = O(\varepsilon_2 \varepsilon_1^2),$$
$$\bar{v}|_{\bar{\eta}=1} = \frac{\partial \bar{h}}{\partial \bar{t}}, \quad \bar{u}|_{\bar{\eta}=1} = 0, \quad \bar{v}|_{\bar{\eta}=0} = 0 \quad \frac{\partial \bar{u}}{\partial \bar{\eta}}|_{\bar{\eta}=0} = 0. \quad (5)$$

If we neglect the $O(\varepsilon_1^2)$ terms, this is of course the system established by Ling and Atabek [16]. Nevertheless, we shall try to get rid of the simplification that they introduced in the expression of the longitudinal gradient: $\bar{u}\frac{\partial \bar{u}}{\partial \bar{x}}$. Having defined accurately the fluid, we now look at the wall. As a complete description is out of our scope, it will be much more simplified than the fluid.

3.3 Final form for the wall

It is difficult to model the artery and all the tissues around it. Often the artery is described as an elastic pipe. For example, a simple shell description is used in Belardinelli and Calvalcanti [2]. A constrained pipe description may be found in Ma, Lee and Wu [17], in Kuiken [10] or in Pedley [23]. This involves of course inertia of the wall, longitudinal tension $\frac{\partial^2 \bar{h}}{\partial \bar{x}^2}$ as well as circumferential tension, viscoelasticity, and careful treatment of the boundary conditions (note that inertia of the wall and nonlinearities may lead to solitary waves: Yomosa [42], Paquerot and Remoissenet [21]). Ohayon and Chadwick [20] noted that the pipe is composed of different non-homogenous media of distinct principal axis, and Teppaz *et al.* [33] include a law in which the shear stress plays a key role. Viscoelasticity may be added as in Horsten *et al.* [12], or in a shell theory as in Moodie *et al.* [19]. If all the non-local effects are neglected, a local law alone may be proposed. Different local laws linking the pressure with the surface were tested by Tardy *et al.* [32], for example their best fit may be written as:

$$\pi(1+\varepsilon_2 h)^2 = \alpha \left(\frac{\pi}{2} + \tan^{-1} \left(\frac{p_0 + \varepsilon_2 p}{\gamma} \right) \right). \quad (6)$$

After inversion, one possible law is $p = F_C(h)$ depending on a set of parameters $C = (\alpha, \gamma, p_0)$. In this paper we use the most simple phenomenological non-linear law:

$$p = kh + k_2 h^2. \quad (7)$$

We assume that the pipe is straight, without any bifurcation and that tapering is negligible. This last effect may be simply introduced by allowing a variating R_0. We may justify this choice if we claim that we study a prosthesis of a femoral artery. As our approach is simple, we may, in the future add other terms:

$$M\frac{\partial^2 h}{\partial t^2} = \left(p - 2\mu \frac{\partial v}{\partial r} \right) - F_C(h) - s\frac{\partial h}{\partial t} - S\frac{\partial^2 h}{\partial x^2},$$

(with $F_C(h) = (kh + k_2 h^2 + k_3 h^3 ...)$, set of parameters $C = (k, k_2, k_3)$ or if $F_C(h)$ is equation (6) then $C = (\alpha, \gamma, p_0)$) and construct the inverse method in order to find the best set of parameters $(C, M, s, S ...)$. These parameters may even depend on x (because of tapering, etc.). Note here, that having adimensionalized the perturbation of pressure by $\varepsilon_2 k R_0$, the pressure-displacement law (7) becomes $\bar{p} = \bar{h} + \bar{k}_2 \bar{h}^2$. Nevertheless, as the elasticity will be one of the parameters which we shall look for, we shall write

$$\bar{p} = \bar{k}_1 \bar{h} + \bar{k}_2 \bar{h}^2, \quad (8)$$

in the following $\bar{k}_1 = 1$ (by construction); except in the last section where we will construct a method to find exactly $\bar{k}_1 = 1$. By definition the compliance is $\partial S/\partial p$, so with our notations:

$$\partial S/\partial p = (2\pi R_0 k^{-1}) \left(\frac{1 + \varepsilon_2 \bar{h}}{1 + (k_2/(k\varepsilon_2))\bar{h}} \right).$$

4 Integral equations

4.1 The equations

Here we adapt Von Kármán integral methods (from aerodynamics Schlichting [29]) to the system (3–4). The key is to integrate the equations with respect to the variable η from the centre of the pipe to the wall ($0 \leq \bar{\eta} \leq 1$). So, we introduce $\bar{U}_0$, the velocity along the axis of symmetry, a kind of loss of flux $\bar{q}$, and $\bar{\Gamma}$ as follows:

$$\bar{U}_0(\bar{x}, \bar{t}) = \bar{u}(\bar{x}, \bar{\eta} = 0, \bar{t}), \quad \bar{q} = \bar{R}^2 \left(\bar{U}_0 - 2\int_0^1 \bar{u}\bar{\eta} \mathrm{d}\bar{\eta} \right)$$
$$\text{and} \quad \bar{\Gamma} = \bar{R}^2 \left(\bar{U}_0^2 - 2\int_0^1 \bar{u}^2 \bar{\eta} \mathrm{d}\bar{\eta} \right). \quad (9)$$

We note that $\bar{q}$ is like the flux difference between a perfect fluid profile and the real one; it is analogous to the displacement thickness δ_1 well known in aerodynamics. $\bar{\Gamma}$ is nearly analogous to the energy displacement thickness δ_2. In aerodynamics the shape factor H links δ_1 and δ_2. Our new unknown functions are q, R and U_0, and we now establish their P.D.E. of evolution. Once again in establishing the fluid motion equation, we suppose that ε_2 is not necessarily too small and $\alpha = O(1)$. The transverse integration of the incompressibility relation (3) with the help of the boundary conditions (5) gives:

$$\frac{\partial \bar{R}^2}{\partial \bar{t}} + \varepsilon_2 \frac{\partial}{\partial \bar{x}} (\bar{R}^2 \bar{U}_0 - \bar{q}) = 0, \quad \bar{R} = 1 + \varepsilon_2 \bar{h}. \quad (10)$$

If we integrate (4), with the help of the boundary conditions (5), we obtain the equation for $q(x,t)$:

$$\frac{\partial \bar{q}}{\partial \bar{t}} + \varepsilon_2 \left(\frac{\partial}{\partial \bar{x}} \bar{\Gamma} - \bar{U}_0 \frac{\partial}{\partial \bar{x}} \bar{q} \right) = -2 \frac{2\pi}{\alpha^2} \tau,$$
$$\tau = \left(\frac{\partial \bar{u}}{\partial \bar{\eta}} \right) |_{\bar{\eta}=1} - \left(\frac{\partial^2 \bar{u}}{\partial \bar{\eta}^2} \right) |_{\bar{\eta}=0}. \quad (11)$$

From the same equation (4) (and from (5)), evaluated on the axis of symmetry (in $\eta = 0$), we obtain an equation for the velocity along the axis $U_0(x,t)$:

$$\frac{\partial \bar{U}_0}{\partial \bar{t}} + \varepsilon_2 \bar{U}_0 \frac{\partial \bar{U}_0}{\partial \bar{x}} = -\frac{\partial \bar{p}}{\partial \bar{x}} + 2 \frac{2\pi}{\alpha^2} \frac{\tau_0}{\bar{R}^2}, \quad \tau_0 = \left(\frac{\partial^2 \bar{u}}{\partial \bar{\eta}^2} \right) |_{\bar{\eta}=0}. \quad (12)$$

The two previous relations introduced the values of the friction in $\eta = 0$, the axis of symmetry: $((\frac{\partial^2 \bar{u}}{\partial \bar{\eta}^2})|_{\bar{\eta}=0})$ and the skin friction in $\eta = 1$, at the wall: $((\frac{\partial \bar{u}}{\partial \bar{\eta}})|_{\bar{\eta}=1})$. Information has been lost here, so we need a closure relation between $(\bar{\Gamma}, \tau, \tau_0)$ and $(\bar{q}, \bar{R}, \bar{U}_0)$. As there are so far no ambiguities, we remove the bars over the adimensionnalized symbols.

4.2 Closure

4.2.1 The selected velocity

As in aerodynamics, the previous system of equations is not closed: we have lost details of the velocity profile in the integration process. Therefore, we have to imagine a velocity profile and deduce from it relations linking Γ, τ and τ_0 and q, U_0 et R. These relations are found from the radial dependence of u. Pohlhausen's idea, explained in Schlichting [29] or Le Balleur [14], consists in postulating an *ad hoc* velocity distribution in η which fits the boundary conditions and "looks like" observed profiles. Here the most simple idea is to use the profiles from the analytical linearized solution given by Womersley [38] for the case with no transverse pressure variation that we have already seen. This solution in complex form ($\mathrm{i}^2 = -1$) is rewritten as:

$$U_{\text{Womersley}} = (F_{\mathrm{W}}(x,t) + \mathrm{i}G_{\mathrm{W}}(x,t))(j_r(\alpha\eta) + \mathrm{i}j_i(\alpha\eta)), \quad (13)$$

where F_{W}, G_{W}, j_{i} and j_{r} are real functions defined as follows:

$$(F_{\mathrm{W}}(x,t) + \mathrm{i}G_{\mathrm{W}}(x,t)) = \frac{kp}{c} \left(1 - \frac{1}{J_0(\mathrm{i}^{3/2}\alpha)} \right) \mathrm{e}^{\mathrm{i}2\pi(t-x/c)},$$
$$(j_{\mathrm{r}} + \mathrm{i}j_{\mathrm{i}}) = \left(\frac{1 - \frac{J_0(\mathrm{i}^{3/2}\alpha\eta)}{J_0(\mathrm{i}^{3/2}\alpha)}}{1 - \frac{1}{J_0(\mathrm{i}^{3/2}\alpha)}} \right).$$

Thus, we will assume that the velocity distribution in the following has the same dependence on η. It means that we suppose that the fundamental mode imposes the radial structure of the flow. The real velocity is:

$$u = 1/2\,((F + \mathrm{i}G)(j_{\mathrm{r}} + \mathrm{i}j_{\mathrm{i}}) + cc) = (Fj_{\mathrm{r}} - Gj_{\mathrm{i}}), \quad (14)$$

where $F(x,t)$ and $G(x,t)$ are now real unknown functions that we want to find and cc is the conjugate complex. We immediately see that $U_0(x,t) = F(x,t)$ (because $j_{\mathrm{r}}(0) = 1$ and $j_{\mathrm{i}}(0) = 0$) and that if we compute q with (14) we obtain $G(x,t)$ as:

$$G(x,t) = \frac{q/R^2 - U_0 + U_0 2 \int_0^1 j_{\mathrm{r}} \eta \mathrm{d}\eta}{2 \int_0^1 j_{\mathrm{i}} \eta \mathrm{d}\eta}. \quad (15)$$

The two functions F and G are only functions of (U_0, R, q) and we keep the Womersley radial dependence.

4.2.2 The coefficients of closure

The velocity at any radius η (14) and (15) may be written with the value of the velocity at the centre U_0 ,the radius R, and the loss of flux q. Next, by integration, we obtain Γ as a function of (U_0, R, q) and, by derivation, we obtain τ and τ_0 as functions of (U_0, R, q):

$$\Gamma = \gamma_{qq} \frac{q^2}{R^2} + \gamma_{qu} q U_0 + \gamma_{uu} R^2 U_0^2,$$
$$\tau = \tau_q \frac{q}{R^2} + \tau_u U_0 \quad \tau_0 = \tau_{0q} \frac{q}{R^2} + \tau_{0u} U_0. \quad (16)$$

This closes the problem. The coefficients $((\gamma_{qq}, \gamma_{qu}, \gamma_{uu}), (\tau_q, \tau_u), (\tau_{0q}, \tau_{0u}))$ are only functions of α. They involve combinations of integrals and derivatives of the Bessel function. For example we have (if $\int f$ is a shorthand for $\int_0^1 f(\eta)\mathrm{d}\eta$ and $\partial_\eta f_{\eta=0}$ an other for $\frac{\partial f}{\partial \eta}(0)$):

$$\gamma_{uu} = 1 - \int j_{\mathrm{i}}^2 / \left(\int j_{\mathrm{i}} \right)^2 - \left(2 \int j_{\mathrm{r}} j_{\mathrm{i}} \right) / \int j_{\mathrm{i}} - \int j_{\mathrm{r}}^2 + \left(2 \int j_{\mathrm{i}}^2 \int j_{\mathrm{r}} \right) / \left(\int j_{\mathrm{i}} \right)^2 + \left(2 \int j_{\mathrm{i}} j_{\mathrm{r}} \int j_{\mathrm{r}} \right) / \int j_{\mathrm{i}} - \left(\int j_{\mathrm{i}}^2 \left(\int j_{\mathrm{r}} \right)^2 \right) / \left(\int j_{\mathrm{i}} \right),$$

$$\tau_{0u} = \partial_\eta^2 j_{\mathrm{r}\eta=0} + \partial_\eta^2 j_{\mathrm{i}\eta=0} / \int j_{\mathrm{i}} - \left(\partial_\eta^2 j_{\mathrm{i}\eta=0} \int j_{\mathrm{r}} \right) / \int j_{\mathrm{i}}.$$

These coefficients are nearly constant for $\alpha < 5$. For α small we obtain from the preceding computations:

$$\left(\left(\frac{-6}{5}, \frac{11}{5}, \frac{-2}{15} \right), (24, -12), (-12, 4) \right), \quad (17)$$

so, we recover the values for the Poiseuille profile at small frequency. The fact that those coefficients are nearly constant makes the model robust. For $\alpha \to \infty$ (in practice,

$\alpha > 12$ is enough) we find from asymptotic behaviour of Bessel functions and from the preceding computations the asymptotic form of the coefficients:

$$\left(\left(\frac{-\alpha}{4\sqrt{2}}, 2, -\frac{\sqrt{2}}{2\alpha}\right),\ (\alpha^2/2, -\alpha\sqrt{2}), (0,0)\right).$$

One can easily show that this is coherent with Wormesley's solution in the limit of large α. We note that for $\alpha \to \infty$ and $\varepsilon_2 = 0$, the wave solution for q is

$$q = \frac{\sqrt{2}}{\alpha\pi}(1-\mathrm{i})\mathrm{e}^{2\mathrm{i}\pi(t-x/x)},$$

$$c = \sqrt{\frac{k}{2}\left(1 - \frac{\sqrt{2}}{\alpha}(1-\mathrm{i}) + O(\alpha^{-2})\right)}.$$

Now equations (8, 10, 11) and (12) with the closure (16) define a set of four monodimensional equations linking the pressure p, the velocity along the axis U_0, the loss of flux q and the variation of the radius h.

4.2.3 Remarks

1- The main difference from other integral methods ([12], [18], [23], [25], [27], [43], [44], or [41] ...) in our approach is the introduction of an auxillary partial differential relation (11) obtained from an aeronautical analogy. Instead of q, Γ and U_0 authors mainly use Q, Q_2 and U_0:

$$Q = \int_0^R 2\pi u r \mathrm{d}r \qquad Q/\pi = U_0 R^2 - q$$

$$Q_2 = \int_0^R 2\pi r u^2 \mathrm{d}r \qquad Q_2/\pi = U_0^2 R^2 - \Gamma.$$

If we substract (10) from (11) we obtain the classical system of two equations:

$$2\pi R\frac{\partial R}{\partial t} + \varepsilon_2 \frac{\partial}{\partial x}(Q) = 0,$$

$$\frac{\partial Q}{\partial t} + \varepsilon_2 \frac{\partial}{\partial x}(Q_2) = -\pi R^2 \frac{\partial p}{\partial x} + \pi\frac{2\pi}{\alpha^2}(\frac{\partial u}{\partial \eta})|_{\eta=1}.$$

Often, the relation for Q_2 is written as $Q_2 = \frac{Q^2}{\pi R^2}$ (in this case the radial variation of the profile is neglected: flat profile) or $Q_2 = \frac{4Q^2}{3\pi R^2}$ (parabolic profile: see Eq. (17)). Note, that we have instead a third differential equation to link Q_1 and Q_2. The effect of the skin friction ($\tau_1 = \frac{2\pi}{\alpha^2}(\frac{\partial u}{\partial \eta})|_{\eta=1}$) is often estimated by $\tau_1 = -\frac{8\pi}{\alpha^2}\frac{Q}{\pi R^3}$, true for a Poiseuille flow only ((17) again). It may be replaced by an unsteady relation (deduced from unsteady Poiseuille flow) such as:

$$T_\tau \frac{\partial \tau_1}{\partial t} + \tau_1 = -\frac{8}{\alpha^2}\left(Q + T_Q\frac{\partial Q}{\partial t} + ...\right).$$

See Yama *et al.* [41] for the derivations and values of coefficients T_τ and T_Q. We do not claim that our description is better, but for a sinusoidal input we find again (at any frequency) the Womersley linear solution. Our profiles are realistic in the sense that they present overshoots in the core and back flow near the wall. This is not the case when the closure is simply $\tau_1 = -\frac{8\pi}{\alpha^2}\frac{Q}{\pi R^3}$ or in the case of very peculiar profiles chosen by Belardinelli and Cavalcanti [2].

2- We noted that the coefficients vary little with α, this shows that our model is very robust: it is easy to see that equations (10, 11) are invariant under the rescaling $t \to t/\Omega$, $/\sqrt{\Omega}$, and $c \to c$, if τ is taken constant (independent of α). This explains why methods based on Poiseuille coefficients are robust too.

5 Numerical resolution of the systems

5.1 Numerical resolution of the boundary layer system

Equations (3–5) are discretized in a simple way: a scheme implicit in (t, η) but explicit in x, first order in time but second order in transversal and longitudinal variables. The non linearity is handled by an internal loop between two time steps (until the maximum of the radius amplitude's variation is smaller than a given small ε, 10^{-5} in practice). The $u\frac{\partial u}{\partial x}$ term has been discretized without any hypothesis and induces no trouble. But, we must keep in mind that boundary layer equations, in the case of a back flow, may lead to a singularity (Van Dommeln and Shen [34]) at a finite time or may present instabilities (Cowley, Hocking and Tutty [5]). Nevertheless, no difficulties were found in the pulsated flow régime for which those equations were settled (ε_2 not too large, α of order 1 to 6).

The boundary condition at the input is only a given displacement h: *i.e.* we impose $h(x_{\mathrm{in}}, t)$. The discrete velocity profile $u(x_{\mathrm{in}}, t)$ is obtained by a simple linear extrapolation from the two next nodes as suggested by Hirsch [11]. The domain is long enough to avoid reflexion at the output, or the output $h(x_{\mathrm{out}}, t)$ is given and the output velocity extrapolated as well.

5.2 Numerical resolution of the integral system

The integral system (10–11) is solved with simple techniques too. It has the form:

$$\frac{\partial f}{\partial t} = \varphi\frac{\partial F}{\partial x} + \sigma,$$

we code it with an Adams Bashford two step method. This scheme is second order in time and space. For the boundary conditions, we follow Hirsch [11], so we impose the displacement at the input and the output ($h(x_{\mathrm{in}}, t)$ and $h(x_{\mathrm{out}}, t)$). The derivatives at the entrance are evaluated upstream and at the output downstream. The fact that the displacement is imposed at both ends permits output impedance problems to be to expelled.

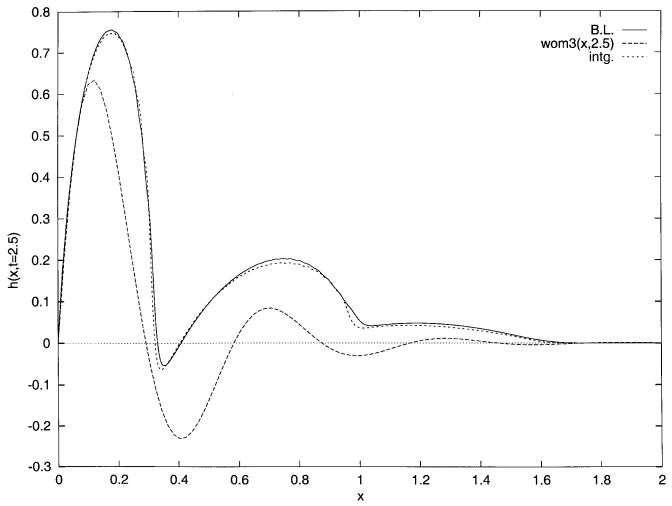

Fig. 2. The displacement of the wall ($h(x, t = 2.5)$) as a function of x is plotted here at time $t = 2.5$. The dashed line (wom3(x,2.5)) is the Womersley solution (reference), the solid line (B.L.) is the result of the Boundary Layer code and the dots (intg) are the results of the integral method ($\alpha = 3$, $k_1 = 1$, $k_2 = 0$ and $\varepsilon_2 = 0.2$).

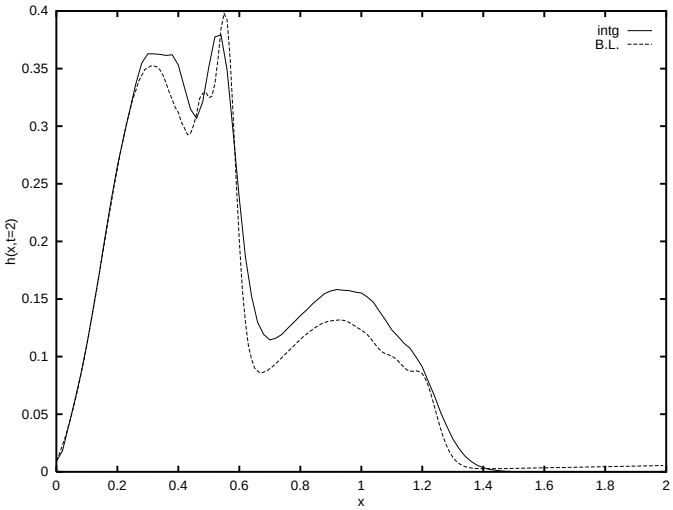

Fig. 3. The displacement of the wall ($h(x, t = 2)$) as a function of x is plotted here at a fixed time $t = 2$. The entrance is the two bumps function. The dashed line (B.L.) is the result of the Boundary Layer code and the solid line (intg) is the result of the integral method ($\alpha = 4$, $k_1 = 1$, $k_2 = 0$ and $\varepsilon_2 = 0.1$).

6 Direct comparisons of the two codes

In this section, the input $h(x_{\rm in}, t)$ is given, the output is far enough to avoid reflexions during the time of computation. The parameters are fixed and are the same for the two codes, $k_1 = 1$ and $k_2 = 0$. The codes were tested in the linearized Womersley solution case ($\varepsilon_2 = 0$).

In Figure 2 we compare the models in the non-linear case ($\alpha = 3$ and $\varepsilon_2 \neq 0$). We observe the nonlinear stiffening of the sinusoid. Increasing ε_2 and α may lead to a shock (Rudinger [28] or Cowley [4]). Our discretisation is not well adapted for shocks, but in rewriting it in a conservative way (with artificial viscosity) it should be possible to catch discontinuities.

To simulate clinical data by thin layer code (3–5) and (7), we put at the entrance a pseudo physiological law which is periodical in t of period 1:

$$h_{\rm in}(t) = 5t{\rm e}^{-100(t-1/6)^2} + 0.5{\rm e}^{-16(t-1/2)^2}. \qquad (18)$$

One example of comparison is in Figure 3.

7 Comparisons of the two resolutions: the inverse method

7.1 Scope of the method

In the preceding sections, we have constructed two models for wave propagation, the second one being a more simplified version of the first, which is itself a huge simplification of the physical problem. The purpose of this paper is to construct an inverse method which will allow the evaluation of the best set of parameters for a model in order to fit experimental data obtained in a non-intrusive way. We suppose that we are able to measure the displacement of the artery at three distinct locations: $x_{\rm in}$, $x_{\rm m}$ and $x_{\rm out}$ (say we have $h_{\rm in}(t)$, $h_{\rm m}(t)$ and $h_{\rm out}(t)$). The computational domain will be $[x_{\rm in}, x_{\rm out}]$, and the measured values are boundary conditions for the computational model: $h(x_{\rm in}, t) = h_{\rm in}(t)$ and $h(x_{\rm out}, t) = h_{\rm out}(t)$. Here, we want to find the values of $k_1 k_2$ and α that give the best agreement between $h(x_{\rm m}, t)$ and $h_{\rm m}(t)$. As we do not have experimental data, the time series $h_{\rm in}(t)$, $h_{\rm m}(t)$ and $h_{\rm out}(t)$ will be produced by the thin layer code.

Following Chavent [3], and taking distances with careful mathematical definitions of the functional spaces, we now build the adjoint problem in order to minimise a cost function. First, we have to define this cost function as an integral criterion which cumulates the errors between $h(x_{\rm m}, t)$ and $h_{\rm m}(t)$ during a time period (of length 1):

$$J = \int_0^1 (h(x_{\rm m}, t) - h_{\rm m}(t))^2 {\rm d}t. \qquad (19)$$

This criterion must be as small as possible. Next, we define a variational formulation of our problem: if we denote (10) as $E_h = 0$, (12) as $E_u = 0$ and (11) as $E_q = 0$, then for any test function h^* u^* and q^* in the *ad hoc* space:

$$E = \int_{x_{\rm in}}^{x_{\rm out}} {\rm d}x(E_{\rm h} h^*) + \int_{x_{\rm in}}^{x_{\rm out}} {\rm d}x(E_u u^*) + \int_{x_{\rm in}}^{x_{\rm out}} {\rm d}x(E_q q^*) \qquad (20)$$

is zero for U_0 q and h solutions of the integral problem (10–11) and (8). Once the variational formulation has been defined, the Lagrangian of the optimization problem is defined by adding criterion (19) to the variational formulation (20) integrated over a time period:

$$\mathfrak{L} = \int_0^1 {\rm d}t(E) + J. \qquad (21)$$

The equations (E_h, E_u and E_q) are here the constraints and (h^* u^* and q^*) are the Lagrangian multiplicators. For any solution $(h(\alpha,k_1,k_2),U_0(\alpha,k_1,k_2),q(\alpha,k_1,k_2))$ of (10–11) and (8), E is zero,

$$E(h(\alpha,k_1,k_2),U_0(\alpha,k_1,k_2),q(\alpha,k_1,k_2))=0$$

and the Lagrangian reduces to the criterion:

$$\mathfrak{L}(h(\alpha,k_1,k_2),U_0(\alpha,k_1,k_2),q(\alpha,k_1,k_2)) = 0+J(h(\alpha,k_1,k_2),U_0(\alpha,k_1,k_2),q(\alpha,k_1,k_2)).$$

By differentiating this last equation we obtain:

$$\delta J=\frac{\partial\mathfrak{L}}{\partial h}\delta h+\frac{\partial\mathfrak{L}}{\partial q}\delta q+\frac{\partial\mathfrak{L}}{\partial U_0}\delta U_0+\frac{\partial\mathfrak{L}}{\partial\alpha}\delta\alpha+\frac{\partial\mathfrak{L}}{\partial k_1}\delta k_1+\frac{\partial\mathfrak{L}}{\partial k_2}\delta k_2. \quad (22)$$

We choose at this point the adjoint variables h^* u^* and q^* such that:

$$\frac{\partial\mathfrak{L}}{\partial h}=0,\ \frac{\partial\mathfrak{L}}{\partial q}=0 \quad \text{and} \quad \frac{\partial\mathfrak{L}}{\partial U_0}=0. \quad (23)$$

This is the adjoint problem that we have to solve. Then equation (22) becomes:

$$\delta J=\frac{\partial\mathfrak{L}}{\partial\alpha}\delta\alpha+\frac{\partial\mathfrak{L}}{\partial k_1}\delta k_1+\frac{\partial\mathfrak{L}}{\partial k_2}\delta k_2. \quad (24)$$

This is the sought expression for the gradient: it depends as well on the direct (10–12) as on the adjoint (25–27) problem.

During manipulations of $\mathfrak{L}$ (22) and (23) the trick is to make integrations by parts, for example terms like $\int\int \mathrm{d}t\mathrm{d}x(\frac{\partial\delta h}{\partial t}h^*)$ are changed into

$$\int\int \mathrm{d}t\mathrm{d}x(-\frac{\partial h^*}{\partial t}\delta h)+\int \mathrm{d}x[\delta h h^*]_{t=0}^{t=1},$$

note that the new system is backward in time ($-\frac{\partial h^*}{\partial t}$). As there is no error in δh at $t=0$, this allows us to fix in a natural way the initial boundary conditions for the back propagation problem such as $h^*(x,t=1)=0$. The same manipulations are done for the spatial derivations leading to the boundary conditions at the edges. Also note when estimating $\delta\mathfrak{L}$ we obtain a source term in the equation of h^* from the cost function differential $\delta\int_0^1 (h(x_\mathrm{m},t)-h_\mathrm{m}(t))^2\mathrm{d}t$, that we write as: $\int_0^1\int_{x_\mathrm{in}}^{x_\mathrm{out}} \delta h\,(\,2(h(x,t)-h_\mathrm{m}(t))\delta_{x_\mathrm{m}}\mathrm{d}x\mathrm{d}t)$, where δ_{x_m} is the Dirac distribution at point x_m.

7.2 The final adjoint system

If we apply the above method with equations (8, 10, 11) and (23),we obtain the following P.D.E., which is the final adjoint system:

$$-2R_0\frac{\partial h^*}{\partial t}-k_1\frac{\partial u^*}{\partial x}-k_2h\frac{\partial u^*}{\partial x}+2(h-h_\mathrm{m})\delta_{x_\mathrm{m}}=0 \quad (25)$$

$$-\frac{\partial u^*}{\partial t}-R_0^2\frac{\partial}{\partial x}(h^*)-\frac{2\,2\pi}{\alpha^2R_0^2}\tau_{0u}u^*+\frac{2\,2\pi}{\alpha^2}(\tau_u q^*)=0 \quad (26)$$

$$-\frac{\partial q^*}{\partial t}+\frac{\partial}{\partial x}(h^*)-\frac{2\,2\pi}{\alpha^2R_0^2}\left(\tau_{0q}\frac{1}{R_0^2}u^*\right)+\frac{2\,2\pi}{\alpha^2}\left(\tau_q\left(\frac{1}{R_0^2}\right)q^*\right)=0. \quad (27)$$

The boundary conditions are for any $x: u^*(x,t=1)=0$, $h^*(x,t=1)=0$, $q^*(x,t=1)=0$, and $h^*(x_\mathrm{in},t)=0$ and $h^*(x_\mathrm{out},t)=0$. The final three components of the gradient (22) of the cost function are:

$$\frac{\partial}{\partial\alpha}J=\iint \mathrm{d}t\mathrm{d}x\left(-\frac{\partial}{\partial\alpha}\left(\frac{2\,2\pi}{\alpha^2R^2}\tau_{0q}\right)\frac{q}{R^2}u^*-\frac{\partial}{\partial\alpha}\left(\frac{2\,2\pi}{\alpha^2R^2}\tau_{0u}\right)U_0u^*+\frac{\partial}{\partial\alpha}\left(\frac{2\,2\pi}{\alpha^2}\tau_q\right)\frac{q}{R^2}q^*+\frac{\partial}{\partial\alpha}\left(\frac{2\,2\pi}{\alpha^2}\tau_u\right)U_0q^*\right) \quad (28)$$

and

$$\frac{\partial}{\partial k_1}J=\iint \mathrm{d}t\mathrm{d}x\left(u^*\frac{\partial h}{\partial x}\right),\quad \frac{\partial}{\partial k_2}J=\iint \mathrm{d}t\mathrm{d}x\left(u^*\frac{\partial h^2}{\partial x}\right). \quad (29)$$

To check the system (25–27) we have found a solution for it in terms of a moving plane linear wave $\mathrm{e}^{-2\mathrm{i}\pi(t-x/c_\mathrm{i})}$. We find that the complex phase velocity c_i is the complex conjugate of the Womersley phase velocity.

7.3 Numerical discretisation

The adjoint system (25–27) is solved using the Adams Bashford method. The Dirac distribution is approximated by a Gaussian function of standard deviation equal to the step size ($\Delta x=0.01$).

A loop of the computation of the gradient is then as follows: first, the input and output come from the thin layer computation (3–5), and starting from $t=0$, $U_0=q=h=0$, we solve (10, 11) and (8) with a given set (α,k_1,k_2), and reiterate until the forced régime is settled (*i.e.* the difference between two periods is less on average than 5×10^{-5}, which is achieved after 6 or 7 periods). All the values during the next period are stored for the gradient's computation. Second, a back propagation computation of (25–27) is performed: the components of the gradient of J (28) and (29) are the results. Third, the values of (α,k_1,k_2) are updated into new ones. For this updating, we tested a simple constant step gradient method and a more sophisticated technique from Press *et al.* [24]. This new set is used for the next loop until convergence: *i.e.* when we approach the minimum of the cost function. The simple constant step method was found to be the more robust. Of course, a great number of iterations is necessary to obtain the minimum.

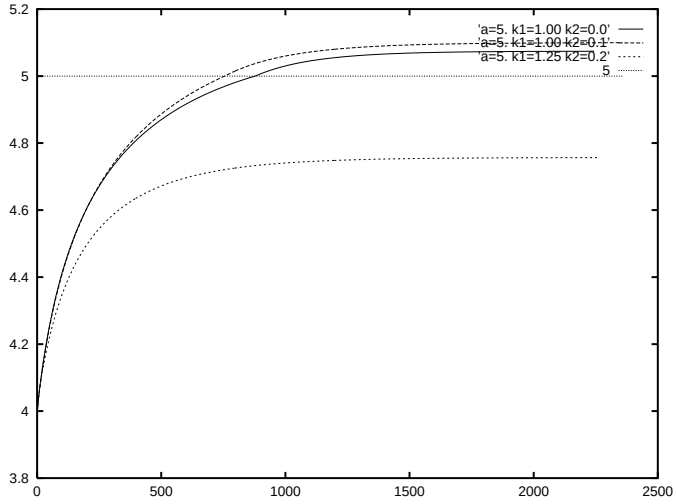

Fig. 4. Variation of α in the three cases as a function of the number of iterations.

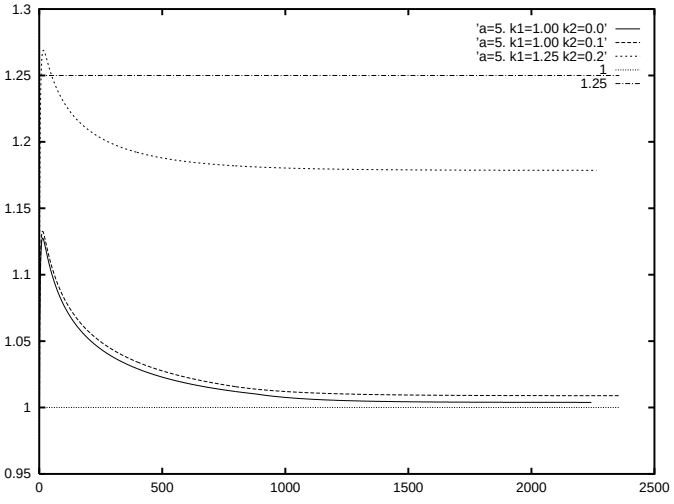

Fig. 5. Variation of k_1 in the three cases as a function of the number of iterations.

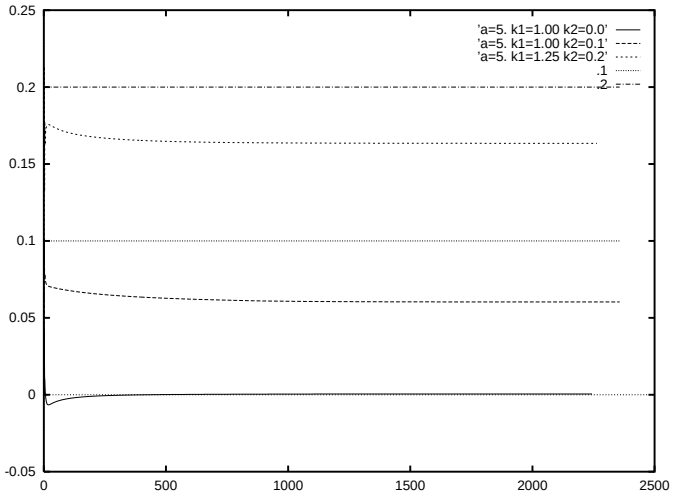

Fig. 6. Variation of k_2 in the three cases as a function of the number of iterations.

7.4 Results

7.4.1 Generation of data

First, we run the boundary layer code (3–5, 7), with an appropriate entry (see below), the output is in 1 where we put $h(1,t) = 0$. This allows reflexions (any other $h(1,t)$ may be imposed, it does not change the result). The input $(h(x_{\rm m},t))$ and two measurements $(h(x_{\rm m},t)$ and $h(x_{\rm out},t))$ are stored after a forced régime has taken place $(t > 4)$. In practice $x_{\rm in} = 0$, and the two values are $x_{\rm m} = 0.12$ and $x_{\rm out} = 0.2$. Of course, particular values for the viscosity and the wall coefficients have been used. Second, we run the backpropagation code to try to retrieve the original values.

7.4.2 Linear wall case with sinusoidal entry

In this full linearized case, (k_2 is imposed to be 0, so we first guess α and k_1) we use at the entry $h_{\rm in}(t) = \sin(2\pi t)$. This is the Womersley problem. About 300 iterations are necessary to obtain the set of parameters. In the range $3 < \alpha < 6$ and $0.7 < k_1 < 2$, the difference between the initially given value and the guessed value is at most 1.5%, the value of k is precise to 0.5%. The agreement, with regard to the numerical errors, is excellent.

7.4.3 Non-linear wall case with sinusoidal entry

In this linearized fluid case ($\varepsilon_2 = 0$) we allow the wall to be non linear $k_2 \neq 0$. Three examples are computed here corresponding to ($\alpha = 5$, $k_1 = 1$, and $k_2 = 0$), ($\alpha = 5$, $k_1 = 1$, and $k_2 = 0.1$) and ($\alpha = 5$, $k_1 = 1.25$, and $k_2 = 0.2$). In Figures 4, 5 and 6 we display respectively the α, k_1 and k_2 history *versus* the number of iterations.

This process is slower (it takes about 1500 iterations to obtain the three parameters). We note that the introduction (in Womersley case) of the new parameter does not affect the precision of α (1.5%) or k_1 (0.4%), the final value of k_2 is 5×10^{-3} (instead of 0). So the agreement is good. If we increase the value of k_2 to 0.1 the error is about 2% for α and less than 1.% for k_1 and the error on k_2 is approximately 0.04. Increasing k_2 to 0.2 gives an error of 5% on α, 5% on k_1 and again the error on k_2 is approximately 0.04. Within the range of the parameters, the absolute error is about 0.2 for α and 0.05 for k_1 and k_2.

7.4.4 Influence of the noise

A simple investigation has been carried out on the influence of noise on the data, a random value lying in the interval [-$\varepsilon_{\rm n}, \varepsilon_{\rm n}$] is added to $h_{\rm in}(t)$, $h_{\rm m}(t)$ and $h_{\rm out}(t)$ in the pure Womersley case. The result of several computations ($\varepsilon_{\rm n} = 0.2$) on the guessed values (α, k_1, k_2) shows that the number of iterations is again nearly around 1500.

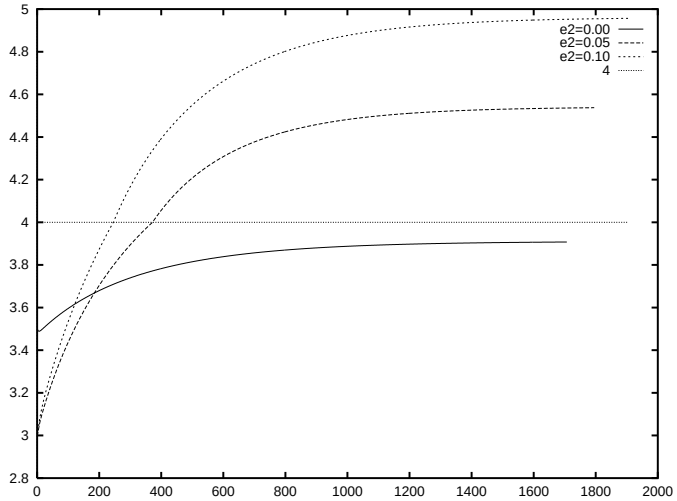

Fig. 7. Variation of α (simulation of $\alpha = 4$, $k_1 = 1.2$ and $k_2 = 0$ and $\varepsilon_2 = 0.1$) with $\varepsilon_2 = 0$, $\varepsilon_2 = 0.05$ and $\varepsilon_2 = 0.1$.

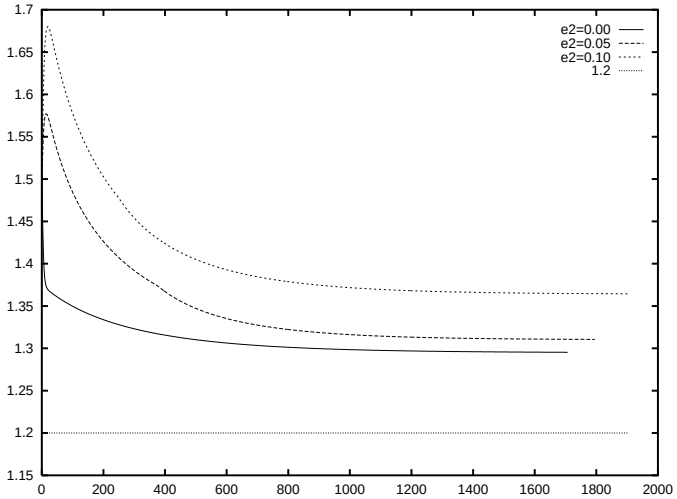

Fig. 8. Variation of k_1 (simulation of $\alpha = 4$, $k_1 = 1.2$ and $k_2 = 0$ and $\varepsilon_2 = 0.1$) with $\varepsilon_2 = 0$, $\varepsilon_2 = 0.05$ and $\varepsilon_2 = 0.1$.

The absolute error is about 0.25 for α, 0.02 for k_1 and 0.01 for k_2.

7.4.5 Linear case physiological

Finally we put at the entry the pseudo physiological law (18). In the linear fluid case $\varepsilon_2 = 0$, the difference on the value of α is about 2.5% and on k about 7.5%. Then if we increase the non-linearities to $\varepsilon_2 = 0.05$ (respectively $\varepsilon_2 = 0.1$), their influence on the result is an error of 13% for α (resp. 24%). In Figures 7 and 8 we see an example of increasing of ε_2.

8 Conclusion

We have presented here a numerical resolution of a set of simplified equations issued from Navier Stokes equation (Ling and Atabek [16]). A simplified integral method, slightly different from the preceding ones, has been presented too. The two methods work fairly well if viscosity or non-linearity are changed (other comparisons should be done using the analytical results from Wang and Tarbel [36,37]). A better comparison has been done in constructing an inverse method: the data from the first code (α, k_1, k_2) were found by the integral method after the resolution of a backpropagation system. Encouraging results are found, even when a small amount of noise is added. This inverse method may be adapted to other sets of simple integral equations and non-linear effects in the fluid may be, in principle, easily added in the description (but will require more computer time anticipating the increase of longitudinal resolution). Of course an inverse method based on (3–5) may be built (anticipating that the power of computers increases). Maybe the results obtained are too simple in comparison to the relative complexity of the inverse method: but while a two parameters try/error shot (only α k_1 with $k_2 = 0$) may be settled without the help of the inverse method, a try/error procedure with 3 parameters is too difficult. The principles of the method were settled for future use: the challenge is now to use real data, obtained by a non-intrusive way, (or numerical data issued from other numerical models) to evaluate mainly the elasticity of the wall. In fact any other phenomena, like a variating k, or a variating R_0 may be added too, opening the way to the detection of stenosis or aneurysm.

The author would like to thank Maurice Rossi (LMM) for discussions. This work was supported by the Direction Supérieure des Programmes Techniques D.S.P.T. 8.

References

1. E. Barros, "Identification de paramètres dans les équations de Saint Venant", Thèse Univ. Paris VI, 1996.
2. E. Belardinelli, S. Cavalcanti, J. Biomech. **25**, 1337 (1992).
3. G. Chavent, "Identification of distributed parameter systems", Proceedings of the 5th IFAC Symposium on Identification and System Parameters Estimations, 1979, pp. 85-97.
4. S.J. Cowley, J.F.M. **116**, 459 (1982).
5. S.J. Cowley, L.M. Hocking, O.R. Tutty, Phys. Fluids **28**, 314 (1985).
6. J.M. Downing, D.N. Ku, J. Biomech. Eng. **119**, 317 (1997).
7. D. Errate, M.J. Esteban, Y. Maday, C. R. Acad. Sci. Paris Ser. I **318**, 275 (1994).
8. P. Flaud, D. Quemada, Rev. Phys. Appl. **15**, 749 (1980).
9. J.M. Fullana, P. Le Gal, M. Rossi, S. Zaleski, Physica D **102**, 37 (1997).
10. G.D.C. Kuiken, J.F.M. **141**, 289 (1984).
11. C. Hirsch, *Numerical computation of internal and external flows* (John Wiley & Sons, 1990) Vol. 2.
12. J.B.A.M. Horsten, A.A. Van Steenhoven, M.E.H. Van Dongen, J. Biomech. **22**, 477 (1989).
13. R.T. Jones, *Blood Flow*, Annual Review of Fluid Mechanics, 1969, pp. 223-243.
14. J.C. Le Balleur, *Viscid- inviscid coupling calculations for 2 and 3D flows*, VKI lecture series 1982-02, 1982.

15. M.J. Lighthill, *Mathematical Biofluiddynamics*, SIAM Philadelphia, 1975.
16. S.C. Ling, H.B. Atabek, J.F.M. **55**, 493 (1972).
17. X. Ma, G.C. Lee, S.G. Wu, J. Biomech. Eng. Trans. ASME **114**, 490 (1992).
18. P. Mederic, R. Gaudu, J. Mauss, M. Zagzoule, Innov. Tech. Biol. Med. **2**, 234 (1991).
19. T.B. Moodie, D.W. Barclay, S.E. Greenwald, D.L. Newman, Acta Mech. **54**, 107 (1984).
20. J. Ohayon, R.S. Chadwick, Biophys. J. **54**, 1077 (1988).
21. J.-F. Paquerot, M. Remoissenet, Phys. Lett. A **194**, 77 (1994).
22. G. Pedrizzetti, J.F.M. **310**, 89 (1996).
23. T.J. Pedley, *The Fluid Mechanics of Large Blood Vessel* (Cambridge University press, 1980).
24. W.H. Press, S.A. Teukolsky, W.T. Vetterling, B.P. Flannery, *Numerical Recipes in C* (Cambridge University Press, 1995).
25. F. Pythoud, N. Stergiopulos, J.-J. Meister, J. Biomech. Eng. **118**, 295 (1996).
26. P.J. Reuderink, F.N. Van de Vosse, A.A. Van Steenhoven, M.E.H. Van Dongen, J.D. Janssen, Int. J. Numer. Methods Fluids **16**, 597 (1993).
27. I. Rogova, P. Flaud, Arch. Physiol. Biochem. **103**, C47 (1995).
28. G. Rudinger, Trans. ASME **5**, 34 (1970).
29. H. Schlichting, *Boundary layer theory* (Mc Graw Hill, 1987).
30. B.R. Seymour, Int. J. Engng. Sci. **13**, 579 (1975).
31. A. Tarantola, *Inverse problem theory* (Elsevier, 1987).
32. Y. Tardy, J.J. Meister, F. Perret, H.R. Brunner, M. Arditi, Clin. Phys. Meas. **12**, 39 (1991).
33. P. Teppaz, R. Herbin, J. Ohayon, Arch. Physiol. Biochem. **103**, C76 (1995).
34. L. Van Dommeln, S.F. Shen, J. Comp. Phys. **38**, 125 (1980).
35. C.C. Vesier, A.P. Yoganathan, J. Comp. Phys. **99**, 271 (1992).
36. D.M. Wang, J.M. Tarbell, J.F.M. **239**, 341 (1992).
37. D.M. Wang, J.M. Tarbell, J. Bio. Mec. **117**, 127 (1995).
38. J.R. Womersley, Philos. Mag. **46**, 199 (1955).
39. S.G. Wu, G.C. Lee, Sci. China **32**, 711 (1989); **106**, 376 (1989).
40. S.G. Wu, G.C. Lee, N.T. Tseng, J. Biomech. Eng. Trans. ASME **106**, 376 (1984).
41. J.R. Yama, P. Mederic, M. Zagzoule, Arch. Physiol. Biochem. **103**, C164 (1995).
42. S. Yomosa, J. Phys. Soc. Jap. **56**, 506 (1987).
43. M. Zagzoule, J. Khalid-Naciri, J. Mauss, J. Biomech. **24**, 435 (1991).
44. M. Zagzoule, J.-P. Marc-Vergnes, J. Biomech. **19**, 1015 (1986).